Agricultural and Forest Meteorology 153 (2012) 31–44

Contents lists available at SciVerse ScienceDirect

Agricultural and Forest Meteorology

journal homepage: www.elsevier.com/locate/agrformet

Energy exchange and evapotranspiration over two temperate semi-arid grasslands in North America

Praveena Krishnan[a,*], Tilden P. Meyers[a], Russell L. Scott[b], Linda Kennedy[c], Mark Heuer[a]

[a] Atmospheric Turbulence and Diffusion Division, NOAA/ARL, Oak Ridge, TN 37830, USA
[b] Southwest Watershed Research Center, USDA-ARS, 2000 E, Allen Road, Tucson, AZ 85719, USA
[c] National Audubon Society, Appleton-Whittell Research Ranch, HC1 Box 44, 366 Research Ranch Road, Elgin, Arizona 85611, USA

ARTICLE INFO

Article history:
Received 6 December 2010
Received in revised form 24 August 2011
Accepted 21 September 2011

Keywords:
Evapotranspiration
Energy exchange
Semi-arid grassland
Eddy covariance
Drought
North American Monsoon

ABSTRACT

The seasonal and interannual variability in surface energy exchange and evapotranspiration (E) of two temperate semi-arid grasslands in southeastern Arizona, USA, were investigated using multi-year (2004–2007) eddy covariance measurements. The study sites, a post-fire site (AG) and an unburned site (KG), received 43–87% of the annual precipitation (P) during the North American Monsoon season (July–September), with the lowest values in the drought years of 2004 and 2005. Irrespective of the differences in temperature, surface albedo, vegetation cover and soil characteristics both sites responded similarly to changes in environmental conditions. The seasonal and interannual variations in the partitioning of net radiation to turbulent fluxes were mainly controlled by P through the changes in soil water content (θ) and vegetation growth. Drastic changes in albedo, vegetation growth and energy fluxes occurred following the onset of the monsoon season in July. During the dry or cool periods of autumn, winter and spring, the sensible heat flux was the largest component of the energy balance, whereas latent heat flux dominated during the warm and wet periods of summer. The dry-foliage Priestley–Taylor coefficient (α) declined when θ in the 0–15 cm soil layer dropped below 0.08 $m^3\ m^{-3}$ at AG, and 0.09 $m^3\ m^{-3}$ at KG, respectively. The July–September average of dry-foliage surface conductance, α and E, reached their lowest values in 2004 at AG and in 2005 at KG. During July–September, monthly E was linearly correlated to the monthly mean θ and the broadband normalized difference vegetation index (NDVI), whereas during May–June the relationship between NDVI and E was not significant. Annual E varied from 264 to 322 mm at AG and from 196 to 284 mm at KG with the lowest value during the severe drought year at the site. July–September E had positive correlation with total P, the mean NDVI and the number of growing season days during that period. Annual P explained more than 80% of the variance in annual E.

1. Introduction

The exchange of energy and water vapor between the land surface and the atmosphere drives the Earth's climate from local to global scales. The partitioning of net radiation into sensible, latent, ground, and surface storage heat fluxes is controlled by factors such as climate, land cover characteristics, hydrological and biochemical processes at the land surface, plant functional type and its phenology, canopy succession stages and boundary layer development (Amiro et al., 2006; Baldocchi, 2003; Wilson et al., 2002a). In addition to natural and anthropogenic disturbances like fire, grazing, harvest and insect defoliation, introduction of non-native species and climate-induced change in vegetation also play an important role in shaping species composition and landscape diversity. This can affect surface albedo and radiation fluxes, leading to a local temperature change and eventually a vegetation response (Pielke et al., 2002). Thus, understanding the relative roles of climate versus vegetation or land cover on energy exchange processes is critical for predicting how ecosystems will respond to future physical and biological perturbations. It is essential to investigate water vapor and energy exchange processes over different ecosystems for multiple years to elucidate the mechanisms that control the water and carbon cycles and other ecosystem processes. Information on seasonal and long-term variations in evapotranspiration (E) has been of particular importance as it is closely linked to ecosystem productivity, water dynamics and regional climate through land surface–atmosphere interactions (Nemani et al., 2002).

Over the past decade, the eddy covariance (EC) method has become a standard tool to study the exchange of carbon, water vapor, and energy between the Earth's surface and atmosphere (Baldocchi, 2003). Although temporal variations in the energy and CO_2 fluxes have been studied extensively for boreal, temperate or

* Corresponding author at: Dept of Commerce, Atmospheric Turbulence and Diffusion Division, NOAA/ARL, 456 South Illinois Avenue, Oak Ridge, TN 37830, USA. Tel.: +1 865 241 2099; fax: +1 865 576 1327.
E-mail address: praveena.krishnan@noaa.gov (P. Krishnan).

0168-1923/$ – see front matter © 2011 Elsevier B.V. All rights reserved.
doi:10.1016/j.agrformet.2011.09.017

tropical forests, grasslands and agricultural ecosystems with little or sporadic drought stress (Meyers, 2001; Hunt et al., 2002; Flanagan et al., 2002; Suyker et al., 2003; Aires et al., 2008) less attention has been given to semi-arid seasonally water-limited ecosystems. Arid and semi-arid ecosystems cover ~40% of the Earth's land surface and therefore are a significant component of Earth's climate system (Moran et al., 1994; White et al., 2000; Novick et al., 2004; Sivakumar et al., 2005; Rotenberg and Yakir, 2010). Changes in the seasonal timing and the amount of rainfall, increased temperatures, and water deficits associated with the projected global climate change are likely to increase arid and semi-arid areas around the world, including the southwestern United States (IPCC, 2007; Seager et al., 2007). As arid grasslands, are very sensitive to changes in available water, regional impacts of global changes are often investigated for these areas threatened by desertification (Kalthoff et al., 2006). In addition to this, grasslands show larger interannual variation in above-ground primary productivity than other biomes in North America in response to changes in precipitation (Knapp and Smith, 2001). Previous studies on the energy, water vapor and CO_2 exchange process over temperate grasslands and agricultural ecosystems (Meyers, 2001; Burba and Verma, 2005; Wever et al., 2002; Suyker and Verma, 2008; Li et al., 2006; Hao et al., 2007), Mediterranean grasslands and mixed oak savannas (Ma et al., 2007; Pereira et al., 2007; Ryu et al., 2008; Xu and Baldocchi, 2004; Baldocchi et al., 2004; Aires et al., 2008), and semi-arid savannas or grasslands (Kurc and Small, 2004; Li et al., 2006; Scott et al., 2009, 2010; Chen et al., 2009; Bowling et al., 2010) have indicated considerable interseasonal and interannual variation in surface energy budget components. However, relatively few studies have been conducted to characterize the quantitative response of energy fluxes and *E* to changes in vegetation and climate over multi-years from semi-arid environments.

In this paper, we examine ~8 site-years of energy and water vapor fluxes over two semi-arid grasslands in southeastern Arizona, United States of America. The study sites include the Audubon and the Kendall grasslands located within 100 km of Tucson, Arizona. The Audubon grassland was completely burned by the Ryan Wildfire (Bock et al., 2007) in April 2002, while the Kendall grassland was unaffected by the fire disturbance. The North American Monsoon (NAM) in this region develops around early July and lasts to mid-September, providing most of the annual rainfall (Adams and Comrie, 1997), which results in dramatic ecosystem response from many biomes in the region. Multi-year EC datasets at the two sites, which included drought (2004 and 2005) and wet years (2006 and 2007), provide a unique opportunity to improve our understanding of the extreme values of energy or water vapor fluxes and related biophysical parameters at these sites. In addition the effects of drought or post-fire recovery if any, on vegetation and its impact on the energy exchange processes can be examined. The changes in phenology and activity of vegetation at the two sites were examined using the broadband normalized difference vegetation index (NDVI), which is a spectral index widely used to characterize temporal and spatial changes in the greenness of vegetated surfaces and in many cases where the vegetation is not too dense, it is often directly related, on a site-specific basis, to leaf area index (LAI) (Qi et al., 2000). Previous studies of the Kendall grassland have focused on the variability, controls and partitioning of *E* (Moran et al., 2009; Nagler et al., 2007; Vivoni et al., 2008; Watts et al., 2007), the evaluation of EC evaporation measurements using watershed water balance (Scott, 2010) and CO_2 exchange (Scott et al., 2010). Observations from the Audubon grassland site have been used for the validation of MODIS land surface temperature products (Wang et al., 2008), estimation of longwave components using ground-based net radiation (Park et al., 2008), and in the inter-comparison of bottom-up and top-down modeling approaches over a variety of vegetative regimes across the Unites States (Houborg et al., 2009). In this paper, we focus mainly on energy partitioning and *E* at the Audubon and Kendall grasslands during 2004–2007. The main objectives of the paper are (1) to examine the seasonal and interannual variation in energy and water vapor fluxes, (2) to determine the effects of the seasonal change in vegetation and soil water conditions on *E* and canopy level biophysical parameters, and (3) to understand the factors controlling the interannual variation in *E*.

2. Materials and methods

2.1. Study sites

The measurements were made in two semi-arid grasslands located ~50 km apart and about 100 km southeast of Tucson, Arizona. The first site, Audubon grassland (hereafter AG), is located on the Appleton-Whittell research ranch (31.5907 N, 110.5104 W, elevation 1496 m), in the Sonoita Valley. The research ranch was established in 1969 as an ecological research preserve, and it is now one of the largest ungrazed, privately managed grassland sites in Arizona (Bock and Bock, 1986). The site naturally regenerated after the Ryan wildfire (Bock et al., 2007) that began on 29 April and continued through 2 May 2002, burning 90% of the standing vegetation and litter on the entire research ranch. The grassland is dominated by warm-temperate, semi-desert grasses including native short-grass prairie (C4 perennial bunchgrasses, primarily *Boutelouagracilis*, *B. curtipendula*, and *Eragrostis intermedia*) and two non-native lovegrasses: Lehmann lovegrass (*Eragrostis lehmanniana*) and Boer lovegrass (*Eragrostis curvula* var. *conferta*). Small woody shrubs (*Mimosa aculeaticarpa* var. *biuncifera*) and perennial herbs (*Astragalus nothoxys*, *Gnaphalium canescens*, *Erigeron* spp. and *Verbena gracilis*) were also scattered on the ranch (McLaughlin and Bowers, 2007). The two African exotic lovegrasses were introduced to the region in the 1940s by the U.S. Soil Conservation Service to control soil erosion and increase forage production on overgrazed rangelands. Vegetation cover in this community was about 65% in 2001 (McLaughlin and Bowers, 2006). Only a small portion of the native grassland remained unburned, but no exotic grassland communities escaped the fire. From 2004 to 2007 the grass canopy cover at the ranch increased from <45% to ~65% and the unvegetated ground decreased from ~45% to 25% (Bock et al., 2011). The grasses reached a maximum height of 0.7 m with a maximum estimated LAI (Wilson and Meyers, 2007) of 1–2.5 $m^2\ m^{-2}$. The soils at AG are Terrarosa complex (fine, mixed, superactive, thermic Ardic Paleustalfs) that consist of deep and well-drained reddish brown sandy clay loams mixed with gravel (with clay and gravel content ranging up to 35%). Based on climate data from the National Climatic Data Center (NCDC) at the Canelo 1NW station (31.56°N, 110.53°W, 1527 m, ~4 km from the site AG), the 1978–2007 mean annual temperature and precipitation were 14.7 °C and 475 mm, respectively.

The second site is the Kendall grassland (31.7365 N, 109.9419 W, elevation 1531 m) (hereafter KG) located in the USDA-ARS Walnut Gulch Experimental Watershed (Scott et al., 2010) near Tombstone, Arizona. The grassland slopes away from the tower at ~10% to the northwest and southeast, at 9% to the southwest and is flat to the northeast over a horizontal distance of ~200 m (Scott, 2010). The grassland was covered mainly by C4 bunchgrasses (*Bouteloua curtipendula*, *Bouteloua eriopoda*, *Bouteloua hirsuta*, *Hilaria belangeri*, and *Aristida hamulosa*) (Weltz et al., 1994), Lehmann lovegrass (*E. lehmanniana*) and C3 shrubs (*Calliadra eriophylla*, *Daleaformosam*, *Krameria parvifolia*, *Prosopis glandulosa*, *Yuccaelata*, and *Isocoma tenuisecta*). The total vegetation cover at the end of growing season was 35%, 17%, and 49% in 2005, 2006, and 2007, respectively, from two vegetation transects near the tower (Scott et al., 2010). Peak leaf area index (LAI) was estimated as ~1 $m^2\ m^{-2}$ with ~40% canopy cover. The grassland was grazed from light to moderate levels throughout this study with minimal visual evidence of heavy

foraging (Scott et al., 2010). The soils at the site are a complex of Stronghold (Coarse-loamy, mixed, thermic Ustollic Calciorthids) and Elgin (Fine, mixed, thermic, Ustollic Paleargids) and generally are very gravelly, sandy to fine sandy loams with clay content ranging from 5% to 15% and slopes ranging from 4% to 9%. The mean annual precipitation and air temperature from 1963 to 2006 was 340 mm and 17 °C, respectively (Moran et al., 2009). Further details on KG are provided in Scott et al. (2010).

2.2. Energy flux and meteorological measurements

Half-hourly turbulent fluxes of sensible heat and water vapor above the canopy were measured continuously using EC technique starting in June 2002 at AG and in May 2004 at KG. The EC instruments at each site were mounted on a tower (at 4 m height at AG and at 9.6 m height at KG up to March 2005 and then at 6.4 m) and consisted of a three-axis sonic anemometer (Model 81000V, RM Young Co., Traverse City, MI at AG, Model CSAT3, Campell Scientific Inc, Logan, UT at KG) and an open-path infrared gas (CO_2/H_2O) analyzer (AG after March 2005 and KG: model LI-7500, LI-COR Inc., Lincoln, NE USA. AG before March 2005: ATDD Open-Path analyzer (Auble and Meyers, 1992)). EC instruments were sampled at 10-Hz using a computer controlled data-logging system. Half-hourly turbulent fluxes were calculated using the covariance of the fluctuations in the vertical wind component and the scalar quantities, namely, air temperature for sensible heat, density of CO_2 for CO_2 flux and density of water vapor for water vapor flux. We also used a two-dimensional coordinate rotation and accounted for the effects of air density fluctuations (Webb et al., 1980) in the calculation of the fluxes. Additional details on sampling procedures and data processing can be found in the works of Meyers (2001) and Scott et al. (2010).

The flux tower at each site was also equipped with instruments to measure the upwelling and downwelling components of photosynthetically active radiation (PAR) (paired quantum sensors, model LI190SA, LI-COR, Lincoln, NE), shortwave radiation (paired pyranometers, model CNR1-CM3, Kipp & Zonen, Delft, The Netherlands), longwave radiation (paired pyrgeometers, CNR1-CG3, Kipp & Zonen, Delft, The Netherlands), wind speed and wind direction (RM Young 05103), pressure (Vaisala PTB101B), air temperature (Thermometrics corp PRT, Northridge, CA) and humidity (Vaisala 50Y, Vaisala Oyj, Helsinki, Finland). Precipitation was measured with a weighing rain gauge at both sites (Hydrol. Serv. TB3 at AG and Belfort at KG). Measurements of soil temperature were made at six depths between 2 and 100 cm with a probe designed in-house that includes YSI Thermistors (model 44034, Measurement Specialties Inc., Hampton, VA at AG). Volumetric soil water content at AG was measured at six depths (10, 20, 30, 40, 60 and 100 cm (Delta-T Devices, Cambridge, U.K.). Volumetric soil water content at KG was measured at 5 and 15 cm depths at three locations using TDR probes (CS616, Campell Scientific). The soil heat flux was measured at 4 cm below the soil surface at AG (Hukseflux Thermal sensors, Delta, The Netherlands, $n = 1$ until December 2005 and then $n = 3$) and at 5 cm below the surface at KG (REBS Inc., Seattle, WA, $n = 3$ till March 2005 and then $n = 5$). Meteorological variables were sampled at intervals of 2 s (using data-logger, model CR23X, Campbell Scientific Inc., Logan, Utah) with averages determined every 30 min. To examine how the tower based Normalized Difference Vegetation Index (NDVI) compare with Moderate Resolution Imaging Spectrometer (MODIS) NDVI, we used 250 m (pixel containing the EC tower) MODIS NDVI time-series data from collection 5 (http://daac.ornl.gov/MODIS/) available as 16-day composite (MOD13Q1) over the periods of 2004–2007. We have also used an estimate of total vegetation cover percentage derived from MODIS data (http://apps.tucson.ars.ag.gov/rdss/index.html).

Table 1
Linear regression coefficients for energy balance closure and the annual ratio of $(H + LE)/(R_n - G - S)$ for the two sites.

Year	Site	Slope	Intercept ($W\,m^{-2}$)	R^2	$\sum(H+LE)/\sum(R_n-G-S)$
2004	AG	0.76	37	0.93	1.26
	KG[a]	0.74	18	0.93	0.93
2005	AG	0.74	35	0.92	1.16
	KG	0.73	24	0.92	1.02
2006	AG	0.77	32	0.93	1.21
	KG	0.71	23	0.92	1.00
2007	AG	0.76	31	0.94	1.01
	KG	0.72	22	0.93	1.01
2004–2007	AG	0.76	31	0.92	1.15
	KG	0.72	22	0.92	0.99

[a] May 7 – December 31, 2004.

The half-hourly turbulent fluxes and meteorological variables were again screened to remove spurious data points that were caused by sensor malfunction, rain/snow events, and sensor maintenance. Small gaps (i.e., <2 h) in the data were filled by linear interpolation. Additional gaps in the meteorological variables of up to 14 days were filled using the mean diurnal variation of the variable. Gaps in net radiation (R_n) at KG were filled using measurements from an additional net radiometer at the site. Longer gaps in sensible (H) and latent heat (λE, where λ is the latent heat of vaporization) fluxes were filled using mean diurnal variation up to 30 days. Additional data gaps in H and daytime λE (nighttime λE value were assumed equal to zero), if any, were filled using the relationship between R_n and H and λE using a moving window of 14 days. The uncertainties in annual E associated with the gap-filling procedure were obtained by resampling the half-hour λE values (1000 times) using Monte Carlo simulation by artificially generating gaps (up to 30% of the total half hours in a year with continuous gaps varying from a half hour to 30 days), using a uniformly distributed random-number generator (Krishnan et al., 2006). From each of the 1000 bootstrap replicates of λE data, the annual values of E were estimated and the 95% confidence level were determined (Table 2).

Before filling the missing data, the annual energy balance closure was evaluated for each site using the linear regressions of the sum of all half-hourly H and λE against $R_n - G - S$, where $G = G_z + \Delta G$, G_z is the measured ground heat flux, ΔG is the ground heat storage above the soil heat flux plates and S is the sum of latent and sensible heat storage in the biomass and air column beneath the EC instrumentation level (Meyers and Hollinger, 2004). Ideal closure is represented by a slope of 1 and an intercept of zero. Slopes of the linear regression at AG ranged from 0.73 to 0.77 and the intercepts varied from 31 to 37 $W\,m^{-2}$. At KG, slopes varied from 0.71 to 0.74 and the intercepts from 18 to 24 $W\,m^{-2}$ (Table 1). The mean slope was 0.76 at AG with 31 $W\,m^{-2}$ intercept ($R^2 = 0.92$) and 0.72 at KG with 22 $W\,m^{-2}$ intercept ($R^2 = 0.92$). The values of the linear regression slope at our study sites were in the range reported for many flux sites (0.53–0.99 with a mean of 0.79) including grasslands and forests (Wilson et al., 2002b) and over short vegetation (0.71–0.91) (Twine et al., 2000). The increase in the slope of the linear regression was 8–17% when ΔG is included and was up to 1% when the S is considered. Annual values of the energy balance ratio were calculated as $\sum(H + \lambda E)/\sum(R_n - G - S)$, which varied from 0.93 to 1.02 at KG and 1.01 to 1.26 at AG and falls with the range (0.39–1.69) of those measured at many other flux sites (Wilson et al., 2002b; Chen et al., 2009; Scott, 2010).

2.3. Additional data analysis

2.3.1. Albedo and NDVI

Albedo was calculated as the ratio of upwelling to downwelling shortwave radiation. A broadband NDVI (Huemmrich

et al., 1999) was calculated as $(R_{NIR} - R_{VIS})/(R_{NIR} + R_{VIS})$, where R_{VIS} denotes the reflectance of the visible radiation (400–700 nm) and R_{NIR} denotes the reflectance of the near-infrared radiation (700–3000 nm). R_{NIR} and R_{VIS} were calculated from the measurements of incident and reflected solar and photosynthetically active radiation (PAR) as described in Wilson and Meyers (2007). The daytime values of albedo and NDVI were calculated by averaging the midday (11:00–14:00 h) values from the above method. The active monsoon growing season (MGS) was delineated as the period between the first and last day of the year when relative NDVI $(=(NDVI - NDVI_{min})/(NDVI_{max} - NDVI_{min})$, where $NDVI_{min}$ and $NDVI_{max}$ are yearly minimum and maximum values, respectively) exceeded 0.5 for at least three consecutive days (White et al., 1997).

2.3.2. Canopy level parameters

To better understand the seasonal and interannual variation in energy fluxes and E and its controlling factors, several canopy-level parameters indicative of ecosystem function were estimated. The effective surface conductance g_s (m s^{-1}) to latent heat transfer was calculated by rearranging the Penman–Monteith equation (Monteith and Unsworth, 1990) to obtain

$$\frac{1}{g_s} = \left[\left(\frac{s}{\gamma}\right)\beta - 1\right]\left(\frac{1}{g_a}\right) + \frac{\rho_a c_p D}{\gamma \lambda E} \quad (1)$$

where s is the rate of change of vapor pressure with temperature in Pa K^{-1}, γ is the psychrometric constant at a given temperature T, in Pa K^{-1}, β is the Bowen ratio ($\beta = H/\lambda E$), g_a is the aerodynamic conductance to heat and mass transfer, ρ_a is the density of air in kg m^{-3}, c_p is specific heat of air in J kg^{-1} K^{-1}, D is the atmospheric saturation deficit in Pa, λ is the latent heat of vaporization of water in J kg^{-1}, and E is the water vapor flux (evapotranspiration) in kg m^{-2} s^{-1}. g_a is given by (Verma, 1989):

$$\frac{1}{g_a} = \frac{u/u_* + 2/k + (\psi_m - \psi_h)/k}{u_*} \quad (2)$$

where k is the von Karman constant (=0.40), and ψ_m and ψ_h are the integral diabatic correction factors for momentum and sensible heat transfer, respectively (Paulson, 1970; Garratt and Francey, 1978). The Priestley–Taylor coefficient (Priestley and Taylor, 1972), which indicates the degree of soil water supply limitation to E was estimated as

$$\alpha = \frac{\lambda E}{\lambda E_{eq}} = \frac{\lambda E}{(s/s+\gamma)R_a} = \frac{s+\gamma}{s(\beta+1)} \quad (3)$$

where E_{eq} is the equilibrium evaporation rate. R_a is the available energy given by $R_a = R_n - G - S$. R_a was replaced by $H + \lambda E$ to avoid the issue of energy-balance non-closure (see Krishnan et al., 2006). Generally, when $\alpha \geq 1$, there is a sufficient supply of soil water so that E is controlled by R_a. The daytime mean dry-foliage g_s, and α were calculated using daytime values when downwelling PAR exceeded 200 μmol m^{-2} s^{-1} for days without precipitation.

3. Results

3.1. Meteorological conditions

The annual cycles of daily mean downwelling shortwave radiation (R_{Sd}), air temperature (T), vapor pressure deficit (D), precipitation (P) and soil water content (θ) in the 0–15 cm layer at AG and KG shown in Fig. 1 indicate that the two sites experienced similar weather with cool winters and warm and wet late summers. R_{Sd}, T and D at both sites increased from winter to midsummer, with the highest values (~350 W m^{-2}, ~30 °C and >3 kPa, respectively) during May–June and then decreased following the onset of the NAM by the first week of July. The precipitation distribution was bimodal, with more than 60% of the annual P received during the NAM period (July–September). The remainder of the rainy season was less well defined and lasted from November to February. Precipitation during winter (December–February) and spring (March–April) periods with dormant vegetation and low evaporative demand resulted in profound changes in θ that even exceeded those during NAM. In general, KG was warmer and drier with high values of D than AG. Both mean annual T and surface temperature (T_s) were higher at KG than at AG by ~2 °C (Table 2) whereas annual P was 34% lower at KG than AG. All years of this study had above-average annual mean temperatures and below-normal annual P at both sites relative to the long-term values (Section 2.1). Although both AG and KG experienced similar weather, there was a noticeable difference in the P distribution between the two sites. The driest year at AG was 2004 with annual P 27% lower than the 4-year (2004–2007) mean (379 (mean) ± 81 (±1 standard deviation) mm). In contrast the driest year at KG was 2005 with annual P 34% lower than the 3-year (2005–2007) mean (250 ± 78 mm). P during the NAM was lower than average in 2004 and 2005 by 55% and 5% respectively, at AG and 12% and 45% respectively, at KG (Table 2). The highest annual P occurred in 2006 at AG and in 2007 at KG. During the severe drought years of 2004 and 2005, θ during the NAM was mostly below 25% of relative water content ($\theta_R = (\theta - \theta_{min})/(\theta_{max} - \theta_{min})$, where θ_{min}, θ_{max} are minimum and maximum values of daily mean θ, respectively excluding the saturation values by the end of 2007).

3.2. Albedo and NDVI

The magnitude and the seasonal variation in shortwave albedo and NDVI were consistently greater at AG than KG (Fig. 2). Shortwave albedo varied between 0.14 and 0.31 at AG and 0.14 and 0.21 at KG. PAR albedo (not shown) followed shortwave albedo, but at AG it varied between 0.05 and 0.23, while at KG it varied between 0.06 and 0.17. Following the onset of NAM and the associated increase in θ, shortwave albedo decreased abruptly and NDVI increased to its peak value by the first week of August, which was almost 1 month after the onset of rainfall due to the delay in biomass production. By the end of September, grass litter and dead biomass were almost golden in color and were highly reflective, resulting in an increase in albedo following senescence. Albedo during MGS was generally low compared with that of winter or autumn periods, which was extremely variable at AG. The 2004–2007 mean albedo at AG (0.21 ± 0.02) was higher than that at KG (0.18 ± 0.01).

The seasonal variation in green biomass as quantified by NDVI (Fig. 2) and the July–September percentage vegetation cover (Table 2) increased from 2004 to 2007. Peak NDVI was the lowest in 2004 due to the extremely dry conditions that affected the vegetation at both sites. In addition to this, the vegetation at AG was not fully recovered from the Ryan fire in 2002. A significant increase in NDVI was observed in 2006 and 2007, with the highest values in 2007 (Table 2). NDVI remained high for longer periods in 2006, the year with the highest July–September P (>80% of the annual P at both sites). Comparison of a 16-day composite of MODIS NDVI and tower NDVI showed good agreement at both sites (NDVI (MODIS) = −0.12 + 1.06 NDVI (tower), $R^2 = 0.74$, $p < 0.0001$ at AG and NDVI (MODIS) = −0.25 + 1.39 NDVI (tower), $R^2 = 0.46$, $p < 0.0001$ at KG). MODIS NDVI showed better agreement with tower NDVI during summer than during winter.

The onset of greenness was apparent from the increase in NDVI following rainfall events during pre-monsoon, monsoon and post-monsoon periods. MGS is the most prominent and persistent growing season (GS) with higher amplitudes of NDVI at these sites. The spring, pre-monsoon (spring, SGS) and post-monsoon growing season are less well defined and can vary depending on the magnitude and distribution of rainfall events during those periods. Onset of MGS following the commencement of NAM is easy to distinguish

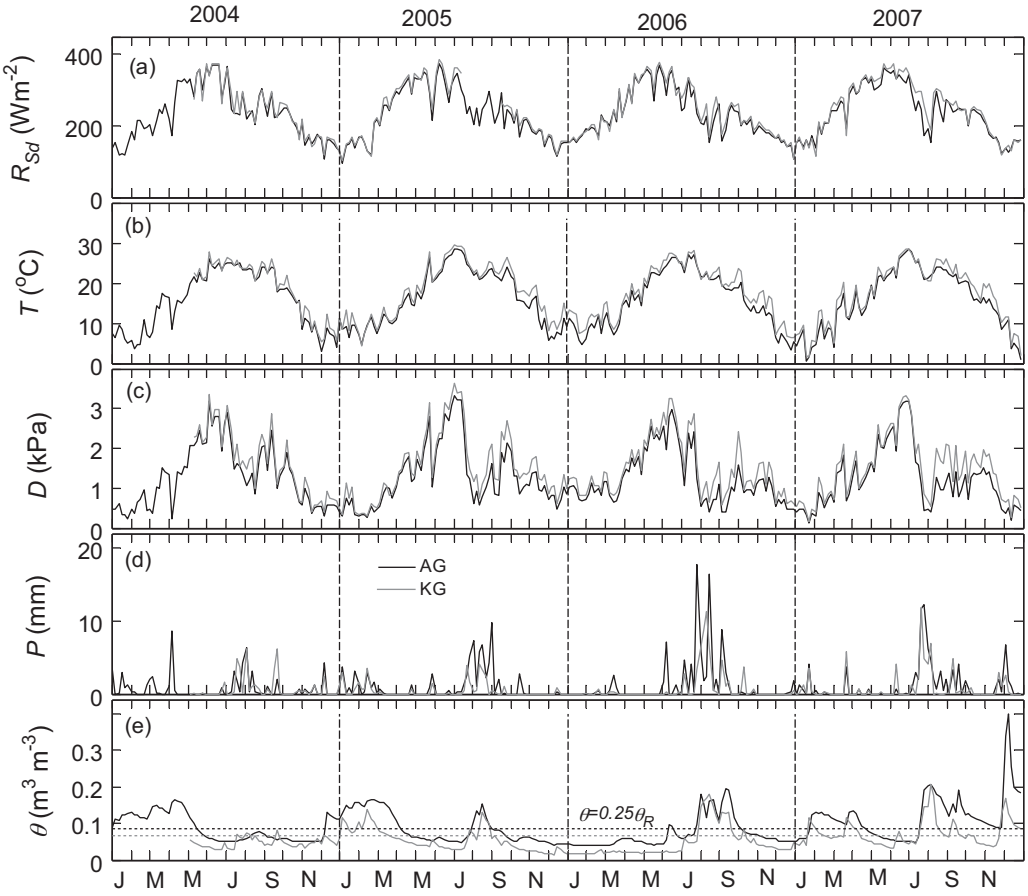

Fig. 1. Five-day averages of daily mean (a) downwelling shortwave radiation (R_{Sd}), (b) air temperature (T), (c) vapor pressure deficit (D), (d) daily total precipitation (P) and (e) soil water content (θ) in the 0–15 cm soil layer at AG and KG. The dark and gray dotted lines in (e) represent θ at 25% of relative water content (θ_R) at AG and KG, respectively. See Section 3.1 for details.

due to the large changes in NDVI, and it is less distinct during the end of the GS. Owing to the lack of daily field observations of grass phenology at both the sites, we inferred the length of the growing season from the seasonal distribution of NDVI (Section 2.3.1). The onset of MGS estimated by this method coincides with the time of the greatest increase in NDVI and the beginning of the CO_2 uptake period. The growing season period calculated by the above method represents the stage of rapid vegetation growth. MGS falls within the time period DOY 209–293 and includes the mid-growing season (DOY 215–285) as defined by Moran et al. (2009), which is the period when the ecosystem is most likely a carbon sink. They reported that perennial plants are likely to be green and transpiring during DOY 180–315. The shortest MGS was in 2004 at AG and in 2005 at KG, the years with the lowest NAM rainfall at the sites (Table 4).

3.3. Components of the surface energy balance

To examine how the seasonal and interannual variation in environmental conditions and phenology affected the partitioning of energy over the grassland, daily mean values of R_n, H, λE and G during 2004–2007 are shown in Fig. 3. Energy fluxes followed roughly

Table 2
Annual values of meteorological and biological variables at AG and KG during 2004–2007.

Site Name	AG				KG			
	2004	2005	2006	2007	2004[a]	2005	2006	2007
Air temperature (°C)	15.6	16.2	15.7	15.7	19.1	17.7	17.4	17.1
Surface temperature (°C)	18.4	19.3	17.9	17.4	21.9	20.3	19.8	20.4
Precipitation (mm)	271	366	458	421	191	162	274	313
Shortwave Albedo	0.19	0.20	0.23	0.21	0.18	0.19	0.18	0.18
Maximum NDVI	0.46	0.52	0.62	0.66	0.40	0.41	0.51	0.57
Net global radiation (W m^{-2})	184	185	175	183	198	193	195	199
Net longwave radiation (W m^{-2})	−126	−125	−121	−116	−106	−126	−122	−123
Evapotranspiration (mm)[b]	264 ± 14	283 ± 17	317 ± 21	322 ± 19	209 ± 14	196 ± 19	211 ± 15	284 ± 16
Length of monsoon growing season (days)[c]	33	63	82	66	57	32	52	33
July–September vegetation cover (%)[d]	32 ± 3	36 ± 6	39 ± 9	43 ± 7	28 ± 2	26 ± 2	30 ± 9	35 ± 9

[a] May 7 – December 31, 2004.
[b] ±95% confidence intervals due to gap-filling. See Section 2 for more details.
[c] See Section 2.3.1 for definition.
[d] Based on MODIS data.

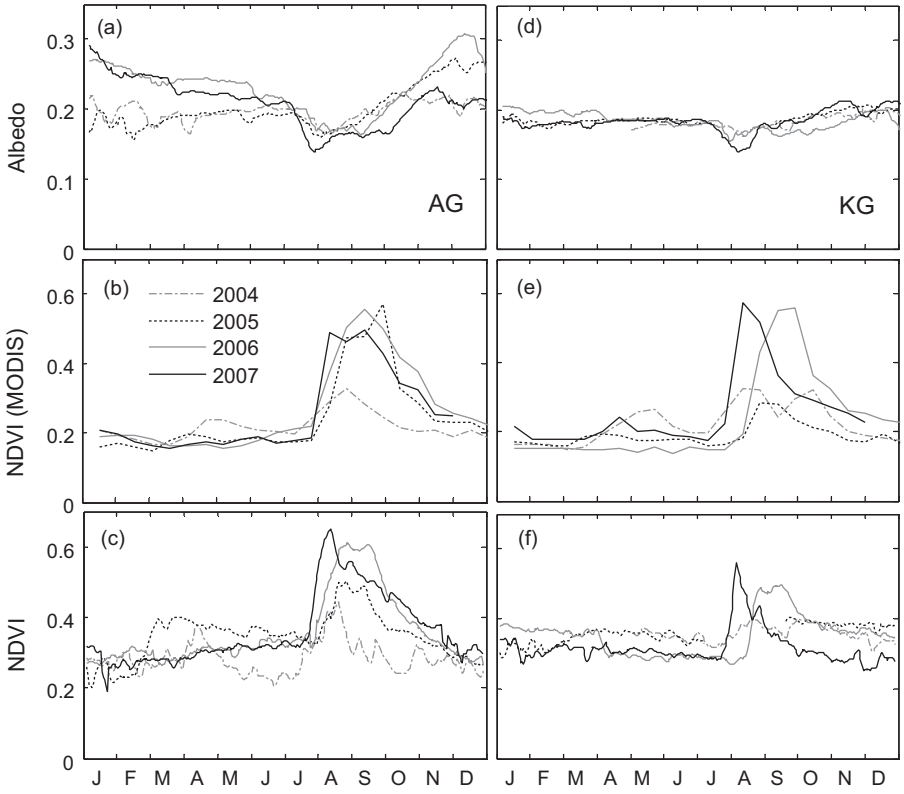

Fig. 2. Five-day running averages of daily midday (1100–1400 h) mean (a and d) shortwave albedo and (c and f) NDVI at AG and KG. (b and e) Shows 16-day composite of MODIS NDVI data for 250 m pixel containing the EC tower, at AG and KG, respectively.

similar seasonal patterns at both the sites. The higher albedo at AG led to lower net shortwave radiation (R_s) (Table 2) and R_n than at KG. However, annual mean net longwave radiation (R_L) at the two sites were similar (-122 ± 4 and $-124 \pm 2\,W\,m^{-2}$ at AG and KG, respectively). The ratio of R_L to R_{Sd} and the ratio of downwelling to upwelling longwave radiation at the sites were about 0.50.and 0.70, respectively.

R_n increased from January to May, reaching $\sim 100\,W\,m^{-2}$ at AG and $\sim 135\,W\,m^{-2}$ at KG during May–June. The decrease in upwelling radiation components (data not shown) following the start of NAM and MGS resulted in an increase in daily mean R_n of up to $50\,W\,m^{-2}$ relative to its pre-monsoon values at both sites. R_n reached the highest values in August. H was typically greater at KG than at AG, consistent with the higher available energy at this site. Both H and G reached peak values during May–June when NDVI values were the lowest. During this time monthly mean midday values of H/R_n increased up to 0.70 from its winter months values of about 0.4. A noticeable change occurred following the onset of NAM and the associated increase in θ and NDVI, resulting in a drop in H/R_n to 0.2 in August. Values of λE increased from nearly zero in winter to $\sim 100\,W\,m^{-2}$ in MGS and accounted for ~40% of R_n during August–September. By the end of the MGS, H/R_n and $\lambda E/R_n$ were nearly equal to the pre-monsoon values. Both λE and G were consistently greater at AG than KG. Even though the magnitude of G was small compared to H and λE (Fig. 3), pre-monsoon and monsoon mean G/R_n reached up to 0.3 at both sites (Table 3). Monthly mean β (data not shown) generally reached values around 10 during May–June and dropped to ~1 during monsoon months. During dry conditions β was >10 with the highest values above 20 during the dry periods of October–November of 2005 and March–May of 2006 at KG. The dry soil conditions and low vegetation growth during August–October of 2004 at AG resulted in above normal values of H/R_n, G, β and below normal values of $\lambda E/R_n$.

Table 3
A comparison of May–June and July–September midday mean values (2004–2007) of shortwave albedo, ratio of sensible, latent and ground heat flux to net radiation (H/R_n, $\lambda E/R_n$, G/R_n, respectively), and Bowen ratio (β) at AG and KG.

Variable	Site	May–June				July–September			
		2004	2005	2006	2007	2004	2005	2006	2007
Albedo	AG	0.21	0.23	0.19	0.20	0.17	0.18	0.18	0.19
	KG	0.18	0.18	0.18	0.18	0.17	0.17	0.18	0.18
H/R_n	AG	0.63	0.63	0.59	0.60	0.52	0.38	0.30	0.35
	KG	0.54	0.59	0.60	0.51	0.45	0.58	0.37	0.38
$\lambda E/R_n$	AG	0.08	0.07	0.09	0.09	0.17	0.27	0.37	0.28
	KG	0.09	0.06	0.02	0.08	0.24	0.22	0.25	0.21
G/R_n	AG	0.24	0.27	0.33	0.30	0.26	0.21	0.22	0.19
	KG	0.23	0.26	0.26	0.30	0.24	0.25	0.25	0.27
β	AG	8.2	10.7	9.9	7.9	3.5	1.8	0.9	2.2
	KG	6.3	11	26	6.3	2.4	3.5	2.2	1.9

Table 4
Interannual variation in July–September air temperature (T, °C), precipitation (P, mm), vapor pressure deficit (D, kPa), soil water content (θ, $m^3\ m^{-3}$) in the 0–15 cm soil layer, NDVI, evapotranspiration (E, mm), dry foliage Priestley–Taylor coefficient (α), surface conductance (g_s, $mm\ s^{-1}$), aerodynamic conductance (g_a, $mm\ s^{-1}$) and maximum daily total E (E_{max}, $mm\ d^{-1}$) at the grasslands.

Variable	AG				KG			
	2004	2005	2006	2007	2004	2005	2006	2007
P	116	244	371	291	146	91	238	188
T	22.9	23.5	21.7	22.7	23.53	24.7	22.8	23.7
D	1.62	1.58	1.07	1.13	1.87	1.98	1.47	1.61
θ	0.06	0.07	0.09	0.11	0.05	0.05	0.07	0.08
NDVI	0.32	0.41	0.48	0.48	0.36	0.38	0.38	0.37
E	99	156	198	177	124	93	145	151
α	0.39	0.584	0.75	0.67	0.47	0.35	0.60	0.51
g_s	1.1	2.3	3.95	3.28	1.4	1.0	3.00	2.05
g_a	7.9	8.45	9.00	9.83	8	9.06	9.43	10.5
E_{max}	2.8	3.5	3.6	3.6	3.1	2.8	3.2	3.6

3.4. Evapotranspiration

The seasonal variation in E corresponded closely with that of P and associated changes in θ and vegetation (Figs. 1 and 4). The highest values of daily E (~2.8–3.6 $mm\ d^{-1}$; Table 4) generally occurred during MGS, especially in August, which was the wettest month with the highest NDVI, R_n, and the lowest D. Annual E varied by ±11% (297 ± 28 $mm\ y^{-1}$) at AG and by ±20% (230 ± 47 $mm\ y^{-1}$) at KG during 2004–2007 and 2005–2007, respectively (Table 2 and Fig. 4). The January-June E consistently exceeded P, resulting in negative P–E by the end of June (Fig. 4). During the rest of the year E was supported by P during the NAM period. There was a noticeable intersite difference in total P and E during NAM, especially in 2004 and 2005. At AG, annual values of E, P–E, July–September E and the peak daily E (264, 7, 99 mm and 2.8 $mm\ d^{-1}$, respectively) were the lowest in 2004, which was the drought year with the lowest NDVI, θ and the shortest MGS (Figs. 1 and 2). At KG, annual values of E, P–E, July–September E and peak daily E (196, −34 and 93 mm and 2.8 $mm\ d^{-1}$, respectively) were the lowest in 2005, which was the drought year at the site with shortest MGS. Annual E in 2004 and 2005 at AG were 12% and 9% lower than the 2004–2007 mean annual E, respectively. At KG, the 2005 annual E was lower than the 3-year mean by 15%. Both sites recorded the highest daily and annual E in 2007, the year with the highest NDVI (Fig. 2). The July–September E contributed up to 40–70% to annual E at both the sites with the lowest values during the drought years and the highest values in 2007 at KG and in 2006 at AG (Table 4). At AG, the January-June E was 27–49% of annual E with the highest value in 2004 whereas at KG it was 12–46% with peak in 2005 (excluding 2004).

There was significant seasonal and interannual variation in α and g_s similar to the changes in E (Figs. 3 and 5). Irrespective of the season, year, and soil water conditions, α decreased non-linearly with a decrease in g_s (Fig. 6) and roughly followed results from theoretical studies on surface E except that α became insensitive to increases in g_s above 6 $mm\ s^{-1}$ instead of the ~16 $mm\ s^{-1}$ found in their results (McNaughton and Spriggs, 1986, 1989). Daily and seasonal mean values (Fig. 3, Table 3) of α were also generally lower than the theoretical maximum value of 1.26 for well watered vegetation (Priestley and Taylor, 1972; McNaughton and

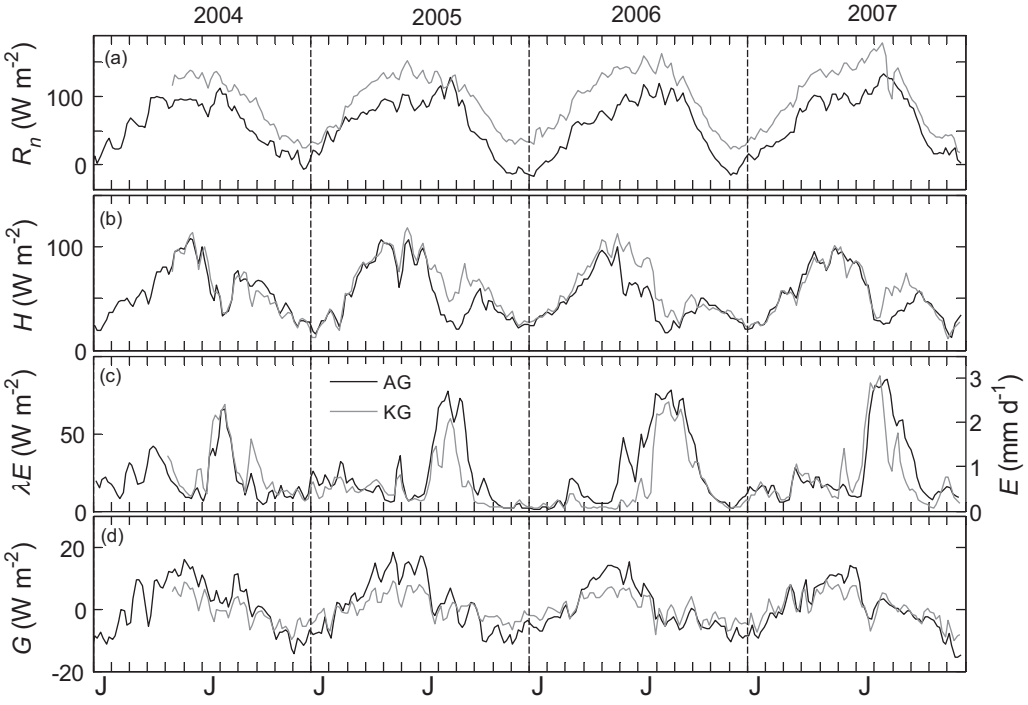

Fig. 3. Five-day running averages of daily (24-h) mean (a) net radiation (R_n), (b) sensible heat flux (H), (c) latent heat flux (λE) or evapotranspiration (E) and (d) ground heat flux (G) at AG and KG during 2004–2007.

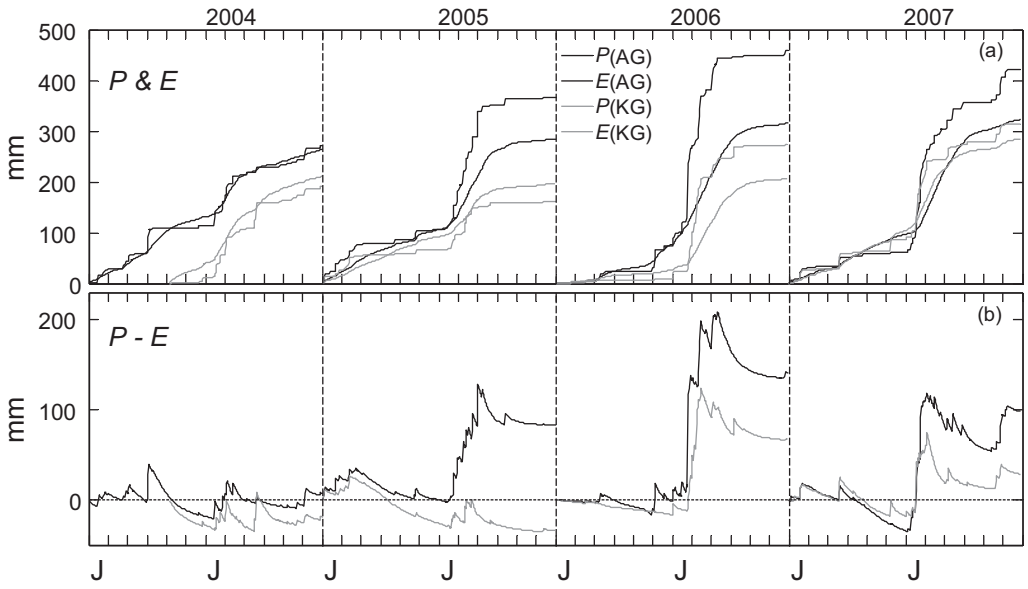

Fig. 4. Annual cycles of cumulative precipitation (P), evapotranspiration (E) and P–E at AG and KG. Data for 2004 at KG during the early part of the year are not provided due to the lack of EC measurements during that period.

Spriggs, 1986). α were >1.1 at AG and ~1 at KG during some periods of July–September, when the canopy was wet and vegetation activity was at its peak. The lowest values of α and g_s typically occurred during dry spring to early summer months as shown in Fig. 5 when D and H were at its highest values (Fig. 3). g_s decreased non-linearly with increasing D (Fig. 7). This effect was most noticeable for $D > 2$ kPa for periods of water stress indicating stomatal control on transpiration. During periods with no shortage of water, g_s appears to be less affected by D. July–September mean α and g_s were higher at AG than KG, except in 2004, which was the drought year at AG. Corresponding to a decline in July–September P by 65% in 2004 at AG, July–September means g_s, α, and E decreased by 65%, 42%, and 44%, respectively, relative to the 2005–2007 values (Table 4). At KG, the decrease in July–September P, g_s, α, and E in 2005 was 52%, 47%, 34% and 33%, respectively. The second lowest values of g_s, α, and E at KG was in 2004, another year with below-normal P.

To assess the influence of daily θ on E, the relationship between α and θ in the 0–15 cm soil layer at the two sites during May–September is shown in Fig. 8. α is often used in comparison studies on the control of daily E by atmospheric and physiological parameters because this ratio normalizes site E values against equilibrium rates primarily determined by R_n. When θ was above a threshold value (θ_T) i.e., 0.08 m^3 m^{-3} ($\theta_R \sim 0.22$) at AG or 0.09 m^3 m^{-3} ($\theta_R \sim 0.33$) at KG, α reached a plateau with values ranging from 0.6 to >1 that were mainly observed during the MGS of 2006 and 2007. However, higher values of α were observed at KG in 2006 and 2007 before the start of MGS but following the onset of NAM. Values of α were nearly zero when θ was ~0.05 m^3 m^{-3} at AG and between 0.02 and 0.05 m^3 m^{-3} at KG. In general, the May–June values of θ were less than θ_T and α followed the same relationship as those during June–September except during the wet periods of May 2004 and June 2006 at AG when $\theta > \theta_T$ and resulted in α values close to 0.4.

Monthly E, α and g_s during July–September at both sites had significant linear correlation with θ ($E = 14.4\theta + 0.27$, $R^2 = 0.67$, $p < 0.001$; $\alpha = 5.19\theta + 0.08$, $R^2 = 0.72$, $p < 0.001$; $g_s = 37.5\theta - 0.98$, $R^2 = 0.73$, $p < 0.001$). An increase in θ had a strong positive effect

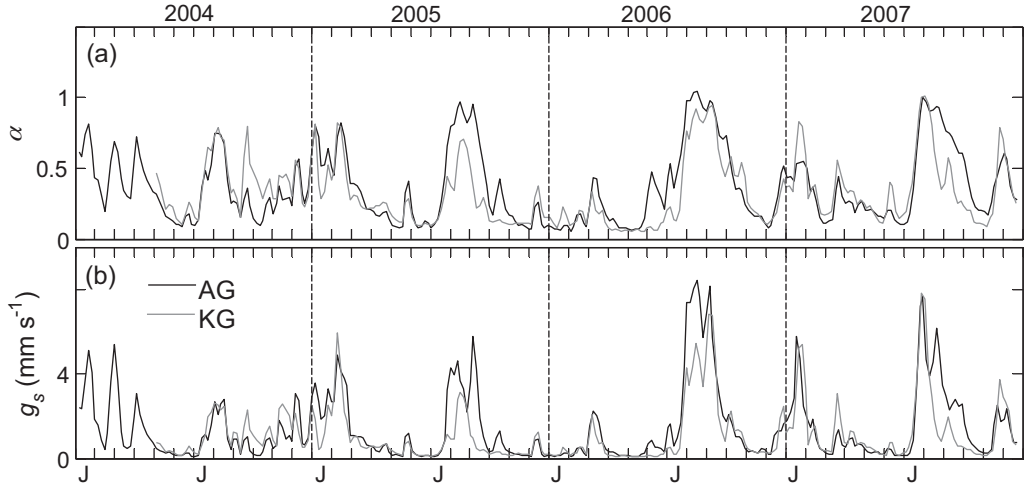

Fig. 5. Five-day running averages of (a) daytime Priestley–Taylor coefficient (α) and surface conductance (g_s) at AG and KG during 2004–2007.

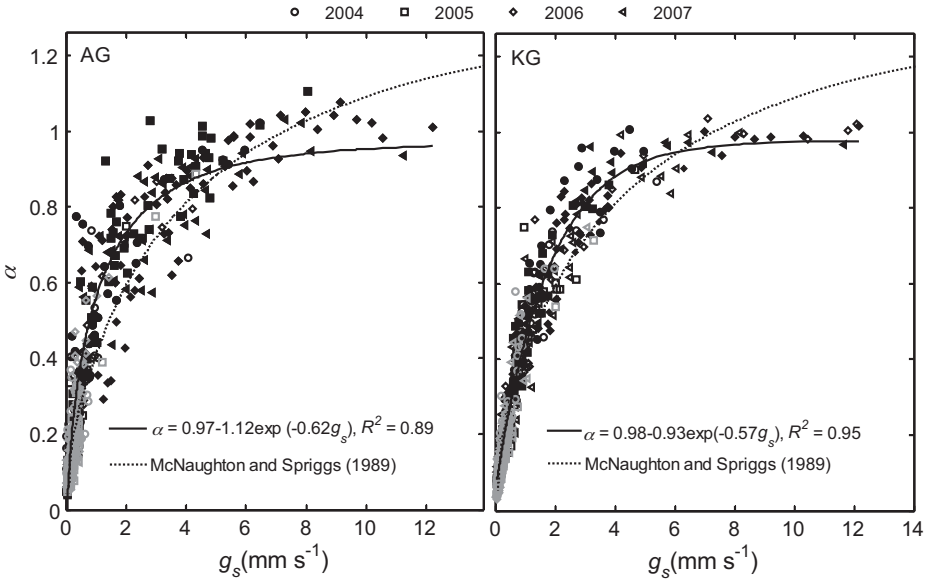

Fig. 6. Relationship between daily mean values of daytime dry-foliage Priestley–Taylor coefficient (α) and surface conductance (g_s) at AG and KG during 2004–2007. Dark and gray symbols represent values during July–September and May–June, respectively. Dark filled symbols denote the monsoon growing season period. The solid curve in each panel represents a fitted regression for data from all years for July–September. For both the sites $\alpha = 0.98 - 1.2\exp(-0.58\,g_s)$, $R^2 = 0.90$, $p < 0.05$. The dotted curve represents the McNaughton and Spriggs (1989) model simulation results as given by Shuttleworth et al. (2009).

on NDVI at both sites (NDVI = $1.83\theta + 0.23$, $R^2 = 0.61$, $p < 0.001$). The relationship between daily values of E and NDVI were not well-defined like in Fig. 8. However, on a monthly basis, E, α and g_s had significant linear relationships with NDVI ($E = 5.72$ NDVI $- 0.72$, $R^2 = 0.59$, $p < 0.001$; $\alpha = 2.17$ NDVI $- 0.31$, $R^2 = 0.69$, $p < 0.001$; $g_s = 37.5$ NDVI $- 0.98$, $R^2 = 0.66$, $p < 0.001$). During May–June, even though the monthly values of θ and E or α or g_s was positively correlated with θ ($E = 8.8\theta + 0.07$, $R^2 = 0.35$, $p < 0.05$; $\alpha = 2.52\theta + 0.05$, $R^2 = 0.32$, $p < 0.05$; $g_s = 3.94\theta + 0.1$, $R^2 = 0.22$, $p < 0.001$), the relationship between NDVI and the above variables were not statistically significant. Similar linear regression analysis of monthly E with T or R_n during May–September showed very weak correlation ($R^2 < 0.07$) indicating that the grasslands were not energy-limited during that period.

3.5. Controls on interannual variation in E

To examine how NDVI, growing season length (GSL) and P influenced the interannual variation in E during NAM, we carried out linear regression analysis as shown in Fig. 9. GSL was defined as the duration of MGS days (see Section 3.2), which fell within July–September period. At both sites, the increase in P, NDVI, and GSL during July–September was positively correlated with July–September E. The relationships between annual P and E were also highly significant ($E = 0.44P + 124$, $R^2 = 0.85$ for both sites). The July–September NDVI explained 41% of the variance in annual E at both sites ($E = 565$ NDVI $+ 36$, $R^2 = 0.41$, $p < 0.08$) and 95% of the variance at AG, whereas this relationship was not significant at KG alone. Even though the GSL correlated well with July–September

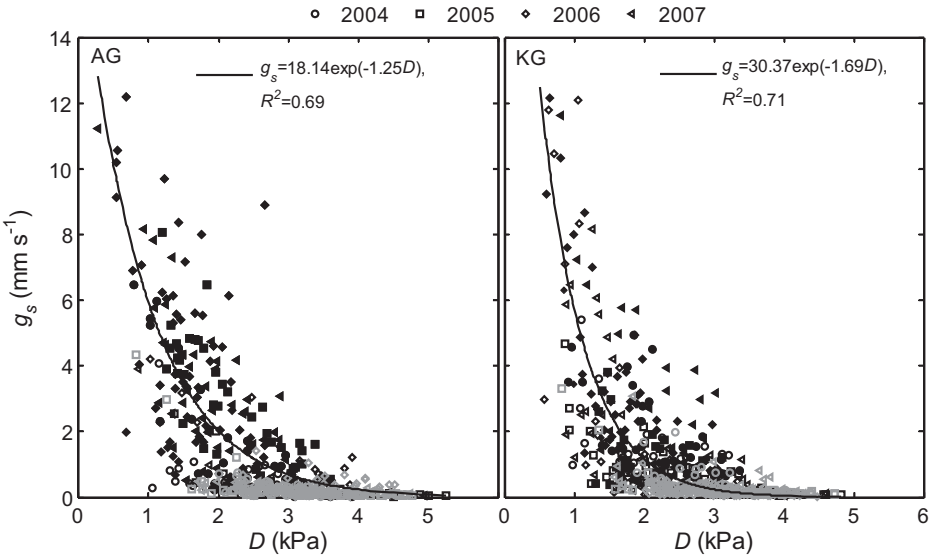

Fig. 7. Relationship between daily mean values of daytime dry-foliage surface conductance (g_s) and vapor pressure deficit (D) at AG and KG. Dark and gray symbols represent values during July–September and May–June, respectively. Dark filled symbols denote the monsoon growing season period. The solid curve in each panel represents a fitted regression for data from all years for July–September. For both the sites $g_s = 17.27\exp(-1.07\,D)$, $R^2 = 0.64$, $p < 0.05$.

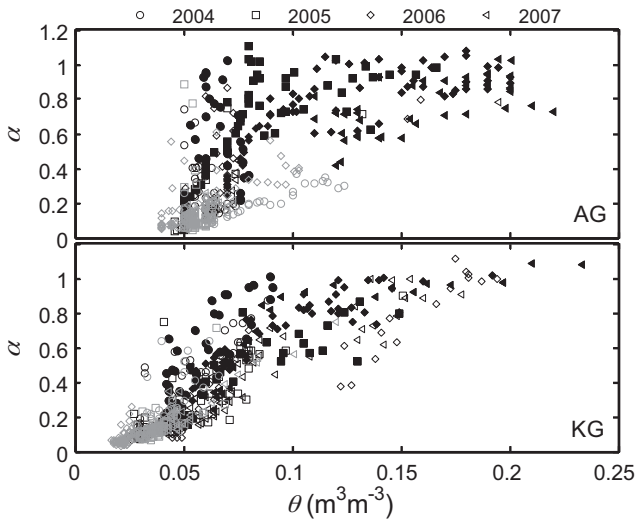

Fig. 8. Relationship between daily mean values of daytime dry-foliage Priestley–Taylor coefficient (α) and soil water content in the 0–15 cm soil layer (θ) at AG and KG. The gray and dark symbols represent data from May–June and July–September periods, respectively. The dark filled symbol denotes values during active monsoon growing season (see text).

E, the relationship between the MGS length (Table 2) on annual *E* was not significant. This suggests that the interannual variation in annual *E* during 2004–2007 was controlled more by annual *P* than July–September NDVI and GSL at both the sites.

4. Discussion

4.1. Partitioning of available energy

Our study indicates that the two semi-arid grasslands responded similarly to environmental conditions, and the interseasonal and interannual differences in energy fluxes were much greater than the intersite differences. The 2004–2007 mean yearly values of R_n/R_{Sd} at AG (25%) and KG (31%) fall within the range of values reported for boreal forests (24–33%) (Baldocchi et al., 2000) but were lower than those values for Mediterranean grassland (33%), Ryu et al., 2008). The mean albedo at KG (Fig. 2, Table 2) was ~11% lower than AG, which led to relatively higher values of R_s and R_n at KG. However, annual mean R_L at the two sites were similar (Table 2) and were well below those reported for boreal, temperate, tropical forests, steppe/semi-arid ecosystems (−96 to −121 W m^{-2}) (Smith et al., 2002; Rotenberg and Yakir, 2010). The higher albedo in early summer and in senescence periods at our study sites could be attributed to surface dryness, bright soils and nonphotosynthetically active vegetation like dormant grasses (Burba and Verma, 2005; Baldocchi et al., 2004). The increase in θ and vegetation growth during the wet monsoon season altered solar heating of the surface via a decrease in albedo likely caused by the darkening of the soil and grass surfaces following rain (Li et al., 2006; Thompson et al., 2004; Montes-Helu et al., 2009; Wang and Davidson, 2009; McFarlane et al., 2009). The impact of albedo on R_n at KG relative to AG is consistent with the studies over forests, shrublands, grasslands, disturbed and undisturbed ecosystems on the effect of changes in albedo on R_n (Liu et al., 2005; Montes-Helu et al., 2009; Baldocchi et al., 2004; Kurc and Small, 2004; Rotenberg and Yakir, 2010). They reported that the higher available energy at low albedo sites generally led to higher values of *H* or λE. In our study, even though R_n and *H* were generally higher at KG, λE was higher at AG, suggesting the role of other environmental variables on energy exchange than the effect of albedo. On average >70% and 30% of annual R_n was used for *H* and λE, respectively. Even though annual *H* at KG exceeded that at AG by ~15%, on a seasonal basis H/R_n during pre-monsoon periods (>0.6) were higher at AG than at KG (Table 3). Values of $\lambda E/R_n$ during peak growing periods (up to 0.4) were similar to a grassland (Aires et al., 2008) but less than the values reported for crops (Suker and Verma, 2008) and tall grass prairie (Burba and Verma, 2005) and were higher than the ratio obtained by Li et al. (2006) for a Mongolian steppe. Annual *G* was almost zero, even though on a seasonal basis (Table 3) G/R_n was up to 0.3, which was generally higher than those reported over grasslands (Aires et al., 2008), but similar to the values over Mongolian steppe (Li et al., 2007). The relatively high contribution of *H* versus λE to R_n, especially at KG, was also evident from the higher values of β (>2 during monsoon and >10 during dry pre-monsoon periods on an average), which is higher than for forest ecosystems ($\beta \sim 1$) (Wilson et al., 2002a; Rotenberg and Yakir, 2010; Teuling et al., 2010). Values of β over grasslands or open fields fluctuate more than over forests, especially during dry conditions with low vegetation (Chen et al., 2009; Stoy et al., 2006). During the severe drought years of 2004 at AG and 2005 at KG, July–September H/R_n and β reached their highest value and $\lambda E/R_n$ reached their lowest values at the site (Table 3). Low values of $\lambda E/R_n$ also suggest the higher sensitivity of λE to changes in environmental conditions.

4.2. Environmental, biophysical and phenological controls on E

Our analysis shows that the magnitude and distribution of *P* controls energy partitioning and *E* through its impact on θ and vegetation in these semi-arid ecosystems. When θ dropped below

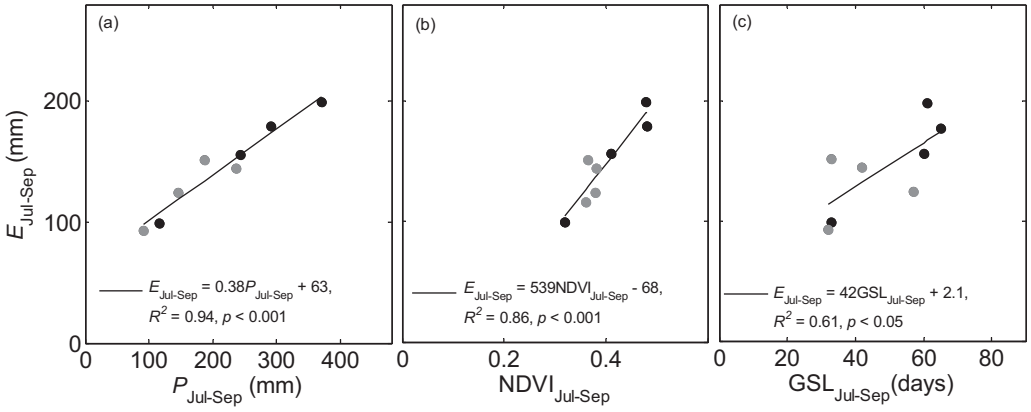

Fig. 9. July–September total evapotranspiration (*E*) as a function of (a) July–September total precipitation (*P*), (b) July–September mean NDVI (c) number of growing season days during July–September, at AG (dark solid circles) and KG (gray solid circles).

θ_T, mainly during the pre-monsoon period or the latter part of the growing season, E declined due to the reductions in g_s associated with soil water stress and high values of D (>2 kPa). The significantly positive relationship between α and g_s, which is consistent with the previous studies over grasslands and forests (Arain et al., 2003; Ryu et al., 2008; Aires et al., 2008) except that α became insensitive to g_s, over 6 mm s^{-1} when compared to >12–16 mm s^{-1} in the above reports, indicated strong surface control on transpiration (McNaughton and Spriggs, 1989). The above relationship and values of α and g_s is also a function of LAI, θ and foliage photosynthetic capacity and can vary with plant functional type (Baldocchi et al., 2004). θ_T at these sites was lower than those reported for other grassland ecosystems, with θ in the range from 10% to 14% (Baldocchi et al., 2004; Kurc and Small, 2004; Aires et al., 2008), suggesting high resilience of these systems to low soil water conditions. The effects of changes in θ on E also depend on the time of the year through the influence by T, R_n, D and LAI (Kelliher et al., 1993; Arain et al., 2003; Baldocchi and Meyers, 1998). During the warm spring and pre-monsoon periods, an increase in θ had a positive effect on E due to high D, whereas during wet NAM periods daily E did not increase with higher values of θ, suggesting the important role of vegetation on E. The influence of vegetation is also evident from the strong correlation between NDVI and g_s or E or α (Section 3.5) consistent with the findings based on LAI (Kelliher et al., 1993; Burba and Verma, 2005; Li et al., 2006). The lack of correlation of E with NDVI during pre-monsoon suggest that evaporation dominated E during that period. But during NAM periods with active vegetation, E comprised mostly of transpiration than evaporation (Nagler et al., 2007). Lower values of E, α and g_s along with high values of D, low NDVI and vegetation cover indicate much drier conditions and higher stomatal limitation on E at KG than AG except in 2004, the drought year at AG.

The timing and magnitude of rainfall is critical at these sites in determining the start and length of growing season. During 2004–2007, the onset of short and less productive SGS (Fig. 2 and Scott et al., 2010) occurred at KG mostly when the cumulative P was above 55 mm which is higher than the threshold of 23 mm for SGS reported by Emmerich and Verdugo (2008). Small signals of SGS were observed at AG in 2004, 2005, and 2007 when the cumulative P was above 104, 80 and 52 mm, respectively. In 2006, winter to pre-monsoon P was less than 20 mm at both sites and did not result in a SGS. The site difference on SGS could be largely due to the changes in species composition and vegetation cover following fire disturbance at AG. Even though the NDVI data captures MGS very well in most of the years, it was difficult to identify SGS based on relative NDVI. Tower NDVI and MODIS NDVI identified the onset of MGS very well, but MODIS NDVI indicated slightly longer MGS than tower NDVI due to differences in the end of the GS. Using a lower threshold (0.3 like in Forzieri et al. (2011) for satellite NDVI), instead of 0.5 in this study increased length of MGS but cannot be applied to the tower NDVI at KG as it included all days following NAM in some years. The onset of NAM, the beginning of MGS, the end of MGS, and the peak NDVI occurred during DOY 197–210, DOY 209–231, DOY 241–293 and DOY 224–239, respectively. Larger variation in the end date of MGS and the positive correlation between θ and NDVI suggest the impact of available soil water in determining the time of transition to senescence. The drought conditions in 2004 at AG and 2005 at KG led to an early senescence, similar to previous reports on drought affected forests and grasslands (Krishnan et al., 2006; Zha et al., 2010). Precipitation events occurred by the end of the MGS, resulting in a post-monsoon GS and delayed senescence at KG in 2004. Even though the onset of MGS was delayed in 2006, the even distribution of P led to a longer GS in 2006. In addition, rapid vegetation activity earlier in the GS (e.g. 2007 at KG with an early MGS) may deplete water faster than slow vegetation activity, resulting in drier and warmer soils, a decrease in g_s and E later in the growing season and an early senescence. Even though the xeric conditions at the end of the GS affected E through the impact of g_s on transpiration in most years, relatively higher D during the end of NAM period maintained E for a longer period of time than the end of the MGS. In contrast to the report by Ryu et al. (2008) that length of GS is the main factor that determines interannual variability of annual E for annual grasslands in California, our study shows that P is the primary factor that controls annual E in these semi-arid grasslands.

Grasslands are more sensitive to the changes in shallow root zone water content than shrublands or forests due to the shallower root system of grasses than forests (Kurc and Small, 2004; Baldocchi et al., 2004; Zha et al., 2010; Tueling et al., 2010). Grasses with a high percentage of their biomass in shallow root systems take better advantage of small precipitation events than deep rooted systems (Cox et al., 1986; Kurc and Small, 2004), especially during SGS. Fire at AG and drought at both sites had an impact on vegetation cover and its composition. Both sites (Section 2.1 and Table 2) showed an increase in vegetation cover in 2006 and 2007. During this time, the grasslands transformed from a native bunch grass community to one dominated by non-native Lehmann lovegrass (Scott et al., 2010 and unpublished data from AG). This could be due to the resilience of Lehmann lovegrass to grazing, drought and fire (Cox et al., 1986) and also its drought resistant seeds that can endure long dry periods and respond more effectively to post drought rainfall compared to most of the native grasses (Emmerich and Hardegree, 1996). Based on a study using microlysimeters at KG for years of similar P, Moran et al. (2009) reported that lovegrass dominance increases the contribution of bare soil evaporation to total E. However, long-term observations at these sites are required to evaluate how the species composition influences seasonal and interannual variation in E and hence energy partitioning.

4.3. Annual E and water balance

The annual E at our study sites during the severe drought years of 2004 and 2005 (264 and 196 mm at AG and KG, respectively) lie in the lower end of range of E (from 163 to 481 mm) reported for grasslands in different climatic zones (Aires et al., 2008; Kurc and Small, 2004; Li et al., 2007; Novick et al., 2004; Ryu et al., 2008; Wever et al., 2002; Zha et al., 2010), whereas E during the other years falls within the middle range. The ratio between E and P can be used as a measure of the "efficiency" of an ecosystem's use of rainfall. In our study E/P varied between 0.72 and 1.2 for all site years and is higher than those for the Mediterranean grasslands (0.4–0.87) (Aires et al., 2008; Ryu et al., 2008) and Mongolian step (0.6) under grazing (Li et al., 2007). Values of E/P peaked during the severe drought years (1.02 and 1.21 at AG in 2004 and at KG in 2005, respectively), similar to the values over temperate grasslands during drought years (Meyers, 2001) and over semi-arid ecosystems (Scott, 2010). On an average, E/P values were higher at KG (0.99 ± 0.20) than at AG (0.84 ± 0.12). The above observations were consistent with the notion that for vegetation to survive in arid conditions, it must make optimum use of the scarce rainfall. E more often exceeded P at KG (Figs. 4), especially during the winter to pre-monsoon periods with high evaporation demand. This pattern of E/P suggests that some portion of P received during the autumn and winter periods was stored in the soil profile and was utilized for E. In general, shallow infiltration in this region (Kurc and Small, 2007; Scott et al., 2009) and small water loss through runoff, which ranges from a fairly small 7% to 12% on an annual basis at the scale of an EC tower footprint (Scott, 2010) at KG indicates that the balance of soil moisture is largely maintained by P and E at this site. Higher seasonal and interannual variations in P–E reflect significant soil water storage changes at the sites, especially at AG (up to 16%), most likely due to the high water holding capacity of the soil at AG

with higher clay content. It is likely that during large rain events water loss through runoff could reach up to 20–30% resulting in lower E/P, mainly during cold months with dormant vegetation and low D. Our study shows that both the magnitude and distribution of P within NAM has a strong impact on the magnitude and interannual variability of annual E. While the even distribution of P during NAM (like in 2006) maintained the MGS for a longer period of time and resulted in higher values of E (up to ~70% of annual E) during the NAM months, P during winter to pre-monsoon months contributed a significant part of annual E especially in drought years (>45% in 2004 at AG and 2005 at KG). As NAM is the dominant and persistent feature in the seasonal cycle which contributes >60% (excluding drought years) of rainfall, E and hence water balance in these grasslands in the long-term are likely to be impacted by the changes in P during the winter to pre-monsoon periods.

5. Conclusions

Multi-year eddy covariance measurements of energy and water vapor fluxes over two temperate semi-arid grasslands in the NAM region of Arizona showed similar seasonal patterns of atmospheric forcing and surface energy partitioning. The lower albedo was responsible for greater R_n at KG than AG, although AG had a lower T_s. The cited difference in R_n led to higher H than λE over KG. Both λE and G were greater at AG, the site with higher P and NDVI, than KG. The interannual and seasonal variation in surface energy partitioning were mainly controlled by P mediated through changes in θ and vegetation At both sites, H consumed the largest fraction of R_n, during periods of limited vegetation growth and dry conditions, whereas λE dominated R_n during wet active growing season periods. Even though G comprised up to 30% of R_n on a seasonal scale, the contribution of annual G to R_n was negligible. Daily α, E and g_s during the growing season were higher at AG than KG, except in 2004. On a monthly scale, both sites had similar and significant linear relationship between θ or NDVI with E, g_s and α during July–September. The strong relationships between α and g_s suggested that during periods of soil water deficit ($\theta < \theta_T$) and high D, the stomatal limitation to transpiration restricted E and hence influenced the surface energy partitioning of the semi-arid grasslands. Associated with the drop in July–September P by 65% at AG in 2004 (47% at KG in 2005), mean g_s and E declined by 65% and 44% (47% and 33%), respectively while β increased by 66% (40%). Even though up to 70% of annual E occurred during NAM, winter to pre-monsoon E, which consistently exceeded P during that period, was a significant component of annual E in some years (>46%, in 2004). Mean annual E accounted for 84% and 99% of annual P at AG and KG, respectively. The main factors that controlled the interannual variation in July–September E at both sites were P, vegetation (as quantified by NDVI) and the number of growing season days during that period, whereas annual E was largely determined by annual P.

Acknowledgements

This work was funded by NOAA's Office of Oceanic and Atmospheric Research, Air Resources Laboratory. This research was performed while P. Krishnan held a National Research Council Research Associateship Award at NOAA. J. Kochendorfer, J. Miller and T. Wilson are acknowledged for internal review of the paper. We also thank the associate editor and two anonymous reviewers for their constructive comments on an earlier version of the manuscript.

References

Adams, D.K., Comrie, A.C., 1997. The North American Monsoon. Bulletin of the American Meteorological Society 78 (10), 7–2114.

Aires, L.M., Pio, C.A., Pereira, J.S., 2008. The effect of drought on energy and water vapor exchange above a Mediterranean C3/C4 grassland in Southern Portugal. Agricultural and Forest Meteorology 148 (4), 565–579.

Amiro, B.D., Barr, A.G., Black, T.A., Iwashitad, H., Kljun, N., McCaughey, J.H., Morgenstern, K., Murayama, S., Nesic, Z., Orchansky, A.L., Saigusa, N., 2006. Carbon, energy and water fluxes at mature and disturbed forest sites, Saskatchewan, Canada. Agricultural and Forest Meteorology 136 (3–4), 237–251.

Arain, M.A., Black, T.A., Barr, A.G., Griffis, T.J., Morgenstern, K., Nesic, Z., 2003. Year-round observations of the energy and water vapor fluxes above a boreal black spruce forest. Hydrological Processes 17 (18), 3581–3600.

Auble, D.L., Meyers, T.P., 1992. An open path, fast response infrared absorption gas analyzer for H_2O and CO_2. Boundary-Layer Meteorology 59 (3), 243–256.

Baldocchi, D., Meyers, T., 1998. On using eco-physiological, micrometeorological and biogeochemical theory to evaluate carbon dioxide, water vapor and trace gas fluxes over vegetation: A perspective. Agricultural and Forest Meteorology 90 (1–2), 1–25.

Baldocchi, D., 2003. Assessing the eddy covariance technique for evaluating carbon dioxide exchange rates of ecosystems: past, present and future. Global Change Biology 9 (4), 479–492.

Baldocchi, D., Kelliher, F.M., Black, T.A., Jarvis, P., 2000. Climate and vegetation controls on boreal zone energy exchange. Global Change Biology 6 (S1), 69–83.

Baldocchi, D., Xu, L., Kiang, N., 2004. How plant functional-type, weather, seasonal an oak-grass savanna and an annual grassland. Agricultural and Forest Meteorology 123 (1–2), 13–39.

Bock, J.H., Bock, C.E., 1986. The Appleton-Whittell Research Ranch Sanctuary of the National Audubon Society. Desert Plants 8, 3–14.

Bock, C.E., Kennedy, L., Bock, J.H., Jones, Z.F., 2007. Effects of fire frequency and intensity on velvet mesquite in an Arizona grassland. Rangeland Ecology and Management 60, 508–514.

Bock, C.E., Jones, Z.F., Kennedy, L.J., Bock, J.H., 2011. Response of rodents to wildfire and livestock grazing in an Arizona desert grassland. American Midland Naturalist 166 (1), 126–138.

Bowling, D.R., Bethers-Marchetti, S., Lunch, C.K., Grote, E.E., Belnap, J., 2010. Carbon, water, and energy fluxes in a semiarid cold desert grassland during and following multiyear drought. Journal of Geophysical Research 115, G04026, doi:10.1029/2010JG001322.

Burba, G.G., Verma, S.B., 2005. Seasonal and interannual variability in evapotranspiration of native tallgrass prairie and cultivated wheat ecosystems. Agricultural and Forest Meteorology 135 (1–4), 190–201.

Chen, S., Chen, J., Lin, G., Zhang, W., Miao, H., Wei, L., Huang, J., Han, X., 2009. Energy balance and partition in Inner Mongolia steppe ecosystems with different land use types. Agricultural and Forest Meteorology 149 (11), 1800–1809.

Cox, J.R, Frasier, G.W., Renard, K.G., 1986. Biomass distribution at grassland and shrubland sites. Rangelands 8, 67–69.

Emmerich, W.E., Verdugo, C.V., 2008. Precipitation thresholds for CO_2 uptake ingrass and shrub plant communities on Walnut Gulch Experimental Watershed. Water Resources Research 44, W05S16, doi:10.1029/2006WR005690.

Emmerich, W.E., Hardegree, S.P., 1996. Partial and full dehydration impact on germination of four warm season grasses. Journal of Range Management 49, 355–360.

Flanagan, L.B., Wever, L.A., Carlson, P.J., 2002. Seasonal and interannual variation in carbon dioxide exchange and carbon balance in a northern temperate grassland. Global Change Biology 8 (7), 599–615.

Forzieri, Giovanni, Fabio Castelli, Enrique, R., Vivoni, 2011. Vegetation dynamics within the North American Monsoon region. Journal of Climate 24, 1763–1783, doi:10.1175/2010JCLI3847.1.

Garratt, J.R., Francey, R.J., 1978. Bulk characteristics of heat transfer in the unstable, baroclinic atmospheric boundary layer. Boundary-Layer Meteorology 15, 399–421.

Huemmrich, K.F., Black, T.A., Jarvis, P.G., McCaughey, J.H., Hall, F.C., 1999. High temporal resolution NDVI phenology from micrometeorological radiation sensors. Journal of Geophysical Research 104 (D22), 27935–27944.

Houborg, R., Anderson, M.C., Norman, J.M., Wilson, T., Meyers, T., 2009. Intercomparison of a bottom-up and top-down modeling paradigm for estimating carbon and energy fluxes over a variety of vegetative regimes across the US. Agricultural and Forest Meteorology.

Hao, Y., Wang, Y., Huang, X., Cui, X., Zhou, X., Wang, S., Niu, H., Jiang, G., 2007. Seasonal and interannual variation in water vapour and energy exchange over a typical steppe in Inner Mongolia. China. Agricultural and Forest Meteorology 146 2007, 57–69.

Hunt, J.E, Kelliher, F.M., McSeveny, T.M., Byers, J.N., 2002. Evaporation and carbon dioxide exchange between the atmosphere and a tussock grassland during a summer drought. Agricultural and Forest Meteorology 111 (1), 65–82.

IPCC, 2007. In: Parry, M.L., Canziani, O.F., Palutikof, J.P., van der Linden, P.J., Hanson, C.E. (Eds.), Climate Change 2007: Impacts, Adaptation and Vulnerability. Contribution of Working Group II to the Fourth Assessment Report of the Intergovernmental Panel on Climate Change. Cambridge University Press, Cambridge, UK, p. 976.

Kalthoff, N., Fiebig-Wittmaack, M., Meissner, C., Kohler, M., Uriarte, M., Bischoff-Gauss, I., Gonzales, E., 2006. The energy balance, evapo-transpiration and nocturnal dew deposition of an arid valley in the Andes. Journal of Arid Environments 65 (3), 420–443.

Kelliher, F.M., Leuning, R., Schulze, E.D., 1993. Evaporation and canopy characteristics of coniferous forests and grasslands. Oecologia 95 (2), 153–163.

Knapp, A.K., Smith, M.D., 2001. Variation among biomes in temporal dynamics of aboveground primary production. Science 291 (5503), 481.
Krishnan, P., Black, T.A., Grant, N.J., Barr, A.G., Hogg, E.T.H., Jassal, R.S., Morgenstern, K., 2006. Impact of changing soil moisture distribution on net ecosystem productivity of a boreal aspen forest during and following drought. Agricultural and Forest Meteorology 139 (3–4), 208–223.
Kurc, S.A, Small, E.E., 2004. Dynamics of evapotranspiration in semiarid grassland and shrubland ecosystems during the summer monsoon season, central New Mexico. Water Resources Research 40, W09305.
Kurc, S.A., Small, E.E., 2007. Soil moisture variations and ecosystemscale fluxes of water and carbon in semiarid grassland and shrubland. Water Resources Research 43, W06416.
Li, S.G., Asanuma, J., Kotani, A., Davaa, G., Oyunbaatar, D., 2007. Evapotranspiration from a Mongolian steppe under grazing and its environmental constraints. Journal of Hydrology 333 (1), 133–143.
Li, S.G., Eugster, W., Asanuma, J., Kotani, A., Davaa, G., Oyunbaatar, D., Sugita, M., 2006. Energy partitioning and its biophysical controls above a grazing steppe in central Mongolia. Agricultural and Forest Meteorology 137 (1–2), 89–106.
Liu, H., Randerson, J.T., Lindfors, J., Chapin Iii, F.S., 2005. Changes in the surface energy budget after fire in boreal ecosystems of interior Alaska: an annual perspective. Journal of Geophysical Research 110 (D13), D13101.
Ma, S., Baldocchi, D.D., Xu, L., Hehn, T., 2007. Inter-annual variability in carbon dioxide exchange of an oak/grass savanna and open grassland in California. Agricultural and Forest Meteorology 147 (3–4), 157–171.
McFarlane, S.A, Kassianov, E.I., Barnard, J., Flynn, C., Ackerman, T.P., 2009. Surface shortwave aerosol radiative forcing during the atmospheric radiation measurement mobile facility deployment in Niamey, Niger. Journal of Geophysical Research 114 (D13).
McLaughlin, S.P., Bowers, J.E., 2006. Plant species richness at different scales in native and exotic grasslands in southeastern Arizona. Western North American Naturalist 66, 209–221.
McLaughlin, S.P., Bowers, J.E., 2007. Effects of exotic grasses on soil seed banks in southeastern Arizona grasslands. Western North American Naturalist 67, 206–218.
McNaughton, K.G., Spriggs, T.W., 1986. A mixed-layer model for regional evaporation. Boundary-Layer Meteorology 34, 243–262.
McNaughton, K.G., Spriggs, T.W., 1989. An evaluation of the Priestley and Taylor equation and the complementary relationship using results from a mixed-layer model of the convective boundary layer. In: paper presented at Estimation of Areal Evapotranspiration, IAHS Publication Vancouver, Canada.
Meyers, T.P., 2001. A comparison of summertime water and CO_2 fluxes over rangeland for well watered and drought conditions. Agricultural and Forest Meteorology 106 (3), 205–214.
Meyers, T.P., Hollinger, S.E., 2004. An assessment of storage terms in the surface energy balance of maize and soybean. Agricultural and Forest Meteorology 125 (1–2), 105–115.
Monteith, J.L, Unsworth, M.H., 1990. Principles of Environmental Physics. Butterworth-Heinemann.
Montes-Helu, M.C., Kolb, T.E., Dore, S., Sullivan, B., Hart, S., Koch, G., Hungate, B., et al., 2009. Persistent effects of fire-induced vegetation change on energy partitioning and evapotranspiration in ponderosa pine forests. Agricultural and Forest Meteorology 149 (3–4), 491–500.
Moran, M.S, Clarke, T.R., Inoue, Y., Vidal, A., 1994. Estimating crop water deficit using the relation between surface-air temperature and spectral vegetation index. Remote Sensing of Environment 49 (3), 246–263.
Moran, M.S., Scott, R.L., Keefer, T.O., Emmerich, W.E., Hernandez, M., Nearing, G.S., Paige, G.B., Cosh, M.H., O'Neill, P.E., 2009. Partitioning evapotranspiration in semiarid grassland and shrubland ecosystems using time series of soil surface temperature. Agricultural and Forest Meteorology 149 (1), 59–72.
Nagler, P.L., Glenn, E.P., Kim, H., Emmerich, W.E., Scott, R.L., Huxman, T.E., 2007. Relationship between evapotranspiration and precipitation pulses in a semiarid rangeland estimated by moisture flux towers and MODIS vegetation indices. Journal of Arid Environments 70 (3), 443–462.
Nemani, R., White, M., Thornton, P., Nishida, K., Reddy, S., Jenkins, J., Running, S., 2002. Recent trends in hydrologic balance have enhanced the terrestrial carbon sink in the United States. Geophysical Research Letters 29 (10), 106–111.
Novick, K.A., Stoy, P.C., Katul, G.G., Ellsworth, D.S., Siqueira, M.B.S., Juang, J., Oren, R., 2004. Carbon dioxide and water vapor exchange in a warm temperate grassland. Oecologia 138 (2), 259–274.
Park, G.H., Gao, X., Sorooshian, S., 2008. Estimation of surface longwave radiation components from ground-based historical net radiation and weather data. Journal of Geophysical Research: Atmospheres 113 (D4), D04207.
Paulson, C.A., 1970. The mathematical representation of wind speed and temperature profiles in the unstable atmospheric surface layer. Journal of Applied Meteorology 9, 857–861.
Pereira, J.S., Mateus, J.A., Aires, L.M., Pita, G., Pio, C., David, J.S., Andrade, V., Banza, J., David, T.S., Pac, T.A., Rodrigues, A., 2007. Net ecosystem carbon exchange in three contrasting Mediterranean ecosystems – the effect of drought. Biogeosciences 4 (5), 791–802.
Pielke, R.A., Marland, G., Betts, R.A., Chase, T.N., Eastman, J.L., Niles, J.O., Niyogi, D.D.S., Running, S.W., 2002. The influence of land-use change and landscape dynamics on the climate system: relevance to climate-change policy beyond the radiative effect of greenhouse gases. Philosophical Transactions A 360 (1797), 1705.
Priestley, C.H.B., Taylor, R.J., 1972. On the assessment of surface heat flux and evaporation using large-scale parameters. Monthly Weather Review 100 (2), 81–92.
Qi, J., Kerr, Y.H., Moran, M.S., Weltz, M., Huete, A.R., Sorooshian, S., Bryant, R., 2000. Leaf area index estimates using remotely sensed data and BRDF models in a semiarid region. Remote Sensing of Environment 73, 18–30, doi:10.1016/S0034-4257(99)00113-3.
Rotenberg, E., Yakir, D., 2010. Contribution of semi-arid forests to the climate system. Science 327 (5964), 451.
Ryu, Y., Baldocchi, D.D., Ma, S., Hehn, T., 2008. Interannual variability of evapotranspiration and energy exchange over an annual grassland in California. Journal of Geophysical Research 113, D09104, doi:10.1029/2007JD009263.
Scott, R.L., 2010. Using watershed water balance to evaluate the accuracy of eddy covariance evaporation measurements for three semiarid ecosystems. Agricultural and Forest Meteorology 150 (2), 219–225.
Scott, R.L, Hamerlynck, E.P., Jenerette, G.D., Moran, M.S., Barron-Gafford, G.A., 2010. Carbon dioxide exchange in a semidesert grassland through drought-induced vegetation change. Journal of Geophysical Research 115 (G3), G03026.
Scott, R.L., Jenerette, G.D., Potts, D.L., Huxman, T.E., 2009. Effects of seasonal drought on net carbon dioxide exchange from a woody-plant-encroached semiarid grassland. Journal of Geophysical Research, 114.
Seager, R., Ting, M.F., Held, I.M., Kushnir, Y., Lu, J., Vecchi, G., Huang, H.-P., Harnik, N., Leetmaa, A., Lau, N.-C., Li, C., Velez, J., Naik, N., 2007. Model projections of an imminent transition to a more arid climate in southwestern North America. Science 316 (5828), 1181.
Shuttleworth, W.J., Serrat-Capdevila, A., Roderick, M.L., Scott, R.L., 2009. On the theory relating changes in area-average and pan evaporation. Quarterly Journal of the Royal Meteorological Society 135, 1230–1247.
Sivakumar, M.V.K., Das, H.P., Brunini, O., 2005. Impacts of present and future climate variability and change on agriculture and forestry in the arid and semi-arid tropics. Increasing Climate Variability and Change, 31–72.
Smith, G.L., Wilber, A.C., Gupta, S.K., Stackhouse Jr., P.W., 2002. Surface radiation budget and climate classification. Journal of Climate 15 (10), 1175–1188.
Stoy, P.C., Katul, G.G., Siqueira, M.B.S., Juang, J.-Y., Novick, K.A., Mccarthy, H.R., Christopher Oishi, A., Uebelherr, J.M., Kim, H.-S., Oren, R., 2006. Separating the effects of climate and vegetation on evapotranspiration along a successional chronosequence in the southeastern US. Global Change Biology 12, 2115–2135.
Suyker, A.E., Verma, S.B., 2008. Interannual water vapor and energy exchange in an irrigated maize-based agroecosystem. Agricultural and Forest Meteorology 148 (3), 417–427.
Suyker, A.E, Verma, S.B., Burba, G.G., 2003. Interannual variability in net CO_2 exchange of a native tallgrass prairie. Global Change Biology 9 (2), 255–265.
Teuling, A.J., Seneviratne, S.I., Stockli, R., Reichstein, M., Moors, E., Ciais, P., Luyssaert, S., van den Hurk, B., Ammann, C., Bernhofer, C., Dellwik, E., Gianelle, D., Gielen, B., Grunwald, T., Klumpp, K., Montagnani, L., Moureaux, C., Sottocornola, M., Wohlfahrt, G., 2010. Contrasting response of European forest and grassland energy exchange to heatwaves. Nature Geoscience 3, 722–727.
Thompson, C., Beringer, J., Chapin III, F.S., McGuire, A.D., 2004. Structural complexity and land surface energy exchange along a gradient from arctic tundra to boreal forest. Journal of Vegetation Science 15 (3), 397–406.
Twine, T.E., Kustas, W.P., Norman, J.M., Cook, D.R., Houser, P.R., Meyers, T.P., Prueger, J.H., Starks, P.J., Wesely, M.L., 2000. Correcting eddy-covariance flux underestimates over a grassland. Agricultural and Forest Meteorology 103 (3), 279–300.
Verma, S., 1989. Aerodynamic resistances to transfers of heat, mass and momentum. In: Paper Presented at Estimation of Areal Evapotranspiration, IAHS Publication, Vancouver, Canada.
Vivoni, E.R., Moreno, H.A., Mascaro, G., Rodriguez, J.C., Watts, C.J., Garatuza-Payan, J., Scott, R.L., 2008. Observed relation between evapotranspiration and soil moisture in the North American Monsoon region. Geophysical Research Letters 35 (22), L22403.
Wang, W., Liang, S., Meyers, T., 2008. Validating MODIS land surface temperature products using long-term nighttime ground measurements. Remote Sensing of Environment 112 (3), 623–635.
Weltz, M. A., J. C. Ritchie, H. D. Fox, (1994), Comparison of laser and field measurements of vegetation height and canopy cover. Water Resources Research 30(5), 1311-1319, doi:10.1029/93WR03067.
Watts, C.J., Scott, R.L., Garatuza-Payan, J., Rodriguez, J.C., Prueger, J., Kustas, W., Douglas, M., 2007. Changes in vegetation condition and surface fluxes during NAME 2004. Journal of Climate 20, 1810–1820.
Webb, E.K., Pearman, G.I., Leuning, R., 1980. Correction of flux measurements for density effects due to heat and water vapor transfer. Quarterly Journal of the Royal Meteorological Society 106, 85–100.
Wever, L.A., Flanagan, L.B., Carlson, P.J., 2002. Seasonal and interannual variation in evapotranspiration, energy balance and surface conductance in a northern temperate grassland. Agricultural and Forest Meteorology 112 (1), 31–49.
White, R.P., Murray, S., Rohweder, M., 2000. Pilot Analysis of Global Ecosystems: Grassland Ecosystems. World Resources Institute.
White, M.A., Thornton, P.E., Running, S.W., 1997. A continental phenology model for monitoring vegetation responses to interannual climatic variability. Global Biogeochemical Cycles 11, 217–234.
Wilson, K., Baldocchi, D., Aubinet, M., Berbigier, P., Bernhofer, C., Dolman, H., Falge, E., Field, C., Goldstein, A., Granier, A., Grelle, A., Halldor, T., Hollinger, D., Katul, G., Law, B., Lindroth, A., Meyers, T., Moncrieff, J., Monson, R., Oechel, W., Tenhunen, J., Valentini, R., Verma, S., Vesala, T., Wofsy, S., 2002a. Energy partitioning between latent and sensible heat flux during the warm season at FLUXNET sites. Water Resources Research 38 (12), 1294, doi:10.1029/2001/WR000989.

Wilson, K., Goldstein, A., Falge, E., Aubinet, M., Baldocchi, D., Berbigier, P., Bernhofer, C., Ceulemans, R., Dolman, H., Field, C., Grelle, A., Ibrom, A., Law, B., Kowalski, A., Meyers, T., Moncrieff, J., Monson, R., Oechel, W., Tenhunen, J., Valentini, R., Verma, S., 2002b. Energy balance closure at FLUXNET sites. Agricultural and Forest Meteorology 113 (1–4), 223–243.

Wilson, T.B., Meyers, T.P., 2007. Determining vegetation indices from solar and photosynthetically active radiation fluxes. Agricultural and Forest Meteorology 144 (3–4), 160–179.

Xu, L., Baldocchi, D., 2004. Seasonal variation in carbon dioxide exchange over a Mediterranean annual grassland in California. Agricultural and Forest Meteorology 123 (1–2), 79–96.

Zha, T., Barr, A.G., Van der Kamp, G., Black, T.A., McCaughey, J.H., Flanagan, L.B., 2010. Interannual variation of evapotranspiration from forest and grassland ecosystems in western Canada in relation to drought. Agricultural and Forest Meteorology 150 (October (11)), 1476–1484.